 Human Molecular Genetics, 2002, Vol. 11, No. 25 3231–3236

SLUG (*SNAI2*) deletions in patients with Waardenburg disease

Manuel Sánchez-Martín[1,†], Arancha Rodríguez-García[1,†], Jesús Pérez-Losada[1], Ana Sagrera[1], Andrew P. Read[2] and Isidro Sánchez-García[1,*]

[1]Instituto de Biología Molecular y Celular del Cáncer (IBMCC), Centro de Investigación del Cáncer, CSIC/Universidad de Salamanca, Campus Unamuno, 37007 Salamanca, Spain and [2]Academic Unit of Medical Genetics, St Mary's Hospital, Manchester M13 0JH, UK

Received August 21, 2002; Revised and Accepted October 4, 2002

Waardenburg syndrome (WS; deafness with pigmentary abnormalities) is a congenital disorder caused by defective function of the embryonic neural crest. Depending on additional symptoms, WS is classified into four types: WS1, WS2, WS3 and WS4. WS1 and WS3 are caused by mutations in *PAX3*, whereas WS2 is heterogenous, being caused by mutations in the *microphthalmia* (*MITF*) gene in some but not all affected families. The identification of *Slugh*, a zinc-finger transcription factor expressed in migratory neural crest cells, as the gene responsible for pigmentary disturbances in mice prompted us to analyse the role of its human homologue *SLUG* in neural crest defects. Here we show that two unrelated patients with WS2 have homozygous deletions in *SLUG* which result in absence of the *SLUG* product. We further show that Mitf is present in Slug-deficient cells and transactivates the SLUG promoter, and that Slugh and Kit genetically interact *in vivo*. Our findings further define the locus heterogeneity of WS2 and point to an essential role of SLUG in the development of neural crest-derived human cell lineages: its absence causes the auditory–pigmentary symptoms in at least some individuals with WS2.

INTRODUCTION

Waardenburg syndrome is a rare (1/40 000) disorder with pigmentary abnormalities and sensorineural deafness, usually inherited in an autosomal dominant manner (1). The main subtypes of WS are type 1 (WS1), associated with dystopia canthorum and type 2 (WS2), without dystopia. WS is a disorder of the neural crest or its derivatives and molecular dissection of WS provides an avenue for investigating neural crest differentiation. WS1 (and the rare type 3 and type 4 variants WS3 and WS4) represent failures of several neural crest derivatives, whereas WS2 appears to be a specific failure of melanocytes. WS1 and WS3 are caused by mutations in *PAX3* (2–4), whereas WS2 is heterogenous (5). Some WS2 families have mutations in the *microphthalmia* (*MITF*) gene and occasional cases are caused by mutations in endothelin 3 or its receptor *EDNRB* (these are more usually associated with Hirschsprung disease in the rare WS4 variant), but for many cases the cause is unidentified. *SLUG* is one possible candidate (6). This zinc finger transcription factor is a marker of neural crest cells in *Xenopus*, zebrafish and chick embryos and probably has a functional role in formation of premigratory neural crest (reviewed in 7). In the mouse, the corresponding gene, *Slugh*, is expressed in migratory but not premigratory neural crest cells and is not essential for neural crest development (7). We recently showed that mice homozygous for loss-of-function mutations of *Slugh* often have a white forehead blaze and areas of depigmentation on the ventral body, tail and feet (6), indicating that the function of Slug is necessary for normal development of melanocytes. Because of the phenotypic similarity of these mice to patients with WS2, we set out to investigate a possible role of the human *SLUG* (*SNAI2*) gene in Waardenburg syndrome.

RESULTS AND DISCUSSION

An initial series of DNAs from 38 unrelated patients, all with features of Waardenburg syndrome [but not necessarily fulfilling the formal diagnostic criteria of Liu *et al.* (8)] and negative for *MITF* mutations, were screened by Southern blotting for *SLUG* gene rearrangements or deletions using a full-length *SLUG* cDNA probe (6). As shown in Figure 1, two subjects showed deletions of *SLUG* spanning the entire *SLUG* coding region. As a control for differences in DNA loading, the blot was stripped and rehybridized with a probe for the *KIT* gene (6), which maps to chromosome segment 4q11–q12. No significant differences in DNA loading were observed with this control probe (Fig. 1C). We tested the extent of the *SLUG*

*To whom correspondence should be addressed. Tel: +34 923238403; Fax: +34 923294813; Email: isg@usal.es
†The authors wish it to be known that, in their opinion, the first two authors should be regarded as joint First Authors.

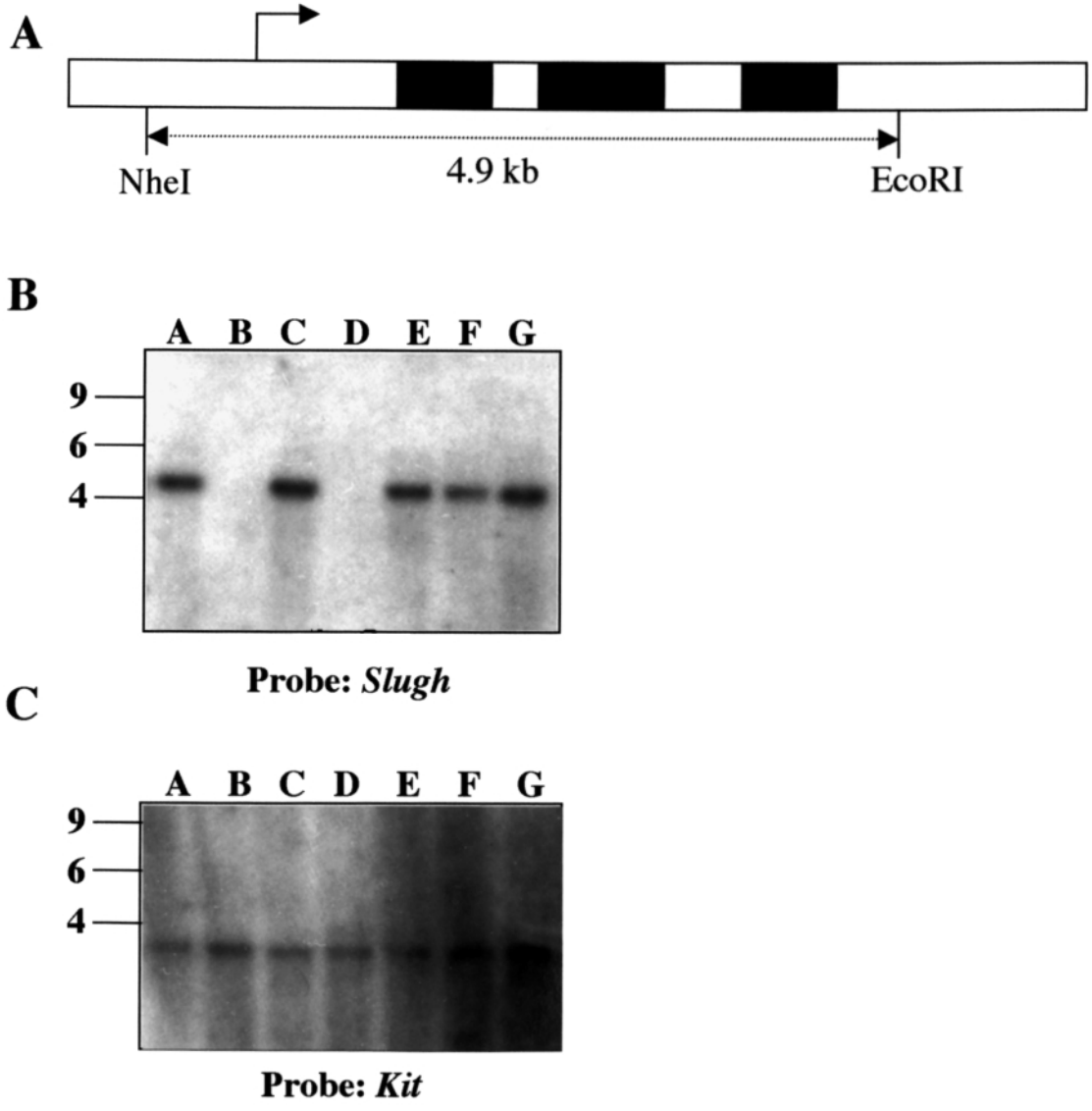

Figure 1. Southern blot hybridization of *SLUG* and *KIT* probes to DNAs from individuals with WS2. Schematic representation of the genomic organization of the human *SLUG* gene with the three exons (**A**). DNAs were cleaved with *Nhe*I and *Eco*RI. The filter was sequentially hybridized to probes for *SLUG* (**B**) and *KIT* (**C**). Size markers are labelled in kb.

Table 1. *SLUG* (*SNAI2*) copy number quantitation by real-time PCR. The Ct is defined as the PCR cycle number at which the fluoresence passes a fixed threshold, which is inversely proportional to the number of target copies present in the sample

	Mice			Subjects				
	$Slug^{+/+}$	$Slug^{+/-}$	$Slug^{-/-}$	A	B	C	D	E
SLUG	23.63 ± 0.1	27.63 ± 0.1	ND	23.29 ± 0.51	ND	23.54 ± 0.36	ND	23.64 ± 0.25
β-Actin	23.44 ± 0.21	23.35 ± 0.9	23.35 ± 0.29	23.59 ± 0.43	23.61 ± 0.23	23.44 ± 0.27	23.29 ± 0.10	23.19 ± 0.24

Ct values ± SEM of triplicate assays are shown. ND, fluorescence not detected.

deletions by analysis of two closely flanking markers, STSG29942 and STSG54511. Both of these markers, which flank the *SLUG* locus, were not homozygously deleted in the two subjects, indicating that the deletions in these patients are relatively short. To confirm these data and accurately determine *SLUG* copy number, we developed a real-time quantitative PCR assay for part of exon 1 of the gene. As shown in Table 1, the target sequence was not detected in subjects B and D, or in $Slugh^{-/-}$ mice. These results thus confirm *SLUG* deletions in subjects B and D.

Figure 2. White spotting phenotype in *Slugh*-deficient mouse. Note areas of hypopigmentation on the midforehead and extrimity depigmentation in a *Slugh*-deficient mice (6,7).

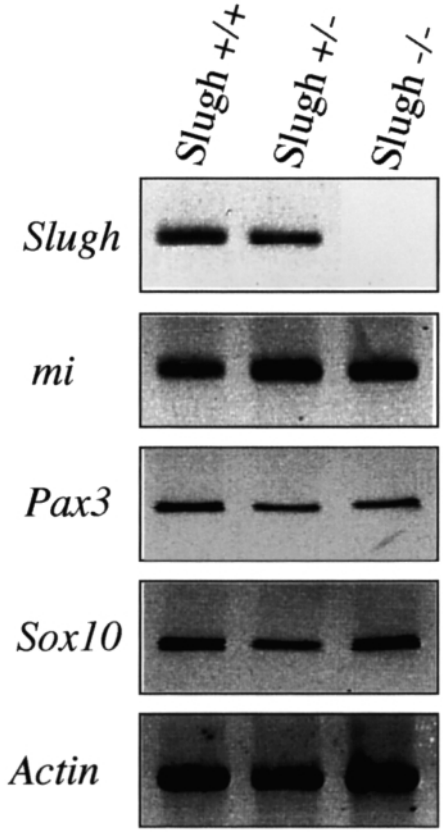

Figure 3. *Pax-3*, *mi* and *Sox10* are expressed in *Slugh*-deficient cells. Expression of *Pax3*, *mi*, *Sox10* and *Slugh* was analysed by RT–PCR in $Slugh^{+/+}$, $Slugh^{+/-}$ and $Slugh^{-/-}$ cells. The PCR products were transferred to a nylon membrane and analysed by hybridization with end-labelled internal oligonucleotide probes specific for each gene. β-Actin was used to check cDNA integrity and loading.

We next searched for point mutations in the *SLUG* gene in the remaining 36 WS2 patients where we did not detect homozygous deletion of the *SLUG* gene. Primers were designed to amplify each coding exon with flanking intron sequence from genomic DNA, and the PCR products were sequenced. We failed to detect any *SLUG* mutations in DNA from the 36 non-deleted patients. Because we have not examined the non-coding part of the gene, it is possible that a more extensive analysis of the entire gene might detect additional mutations in our panel of patients. The possibility of a population polymorphism was excluded as we detect no *SLUG* deletions in 150 controls studied.

Patients were not selected for any particular mode of inheritance. Of the 38, 13 had a clearly dominant family history, 12 (including the two deletion cases) had pedigrees fully compatible with recessive inheritance and 13 were classified as possible recessive. The 'possibly recessive' category included patients where a parent or more distant relative was reported to have some minor pigmentary change such as early graying or a white forelock. In some cases patients with similar histories have turned out to be homozygous for connexin 26 mutations (A.P.R., unpublished), showing that such pedigrees can be compatible with recessive inheritance. Connexin 26 mutations were excluded in our patients.

Subject B was a 15-year-old girl of Bangladeshi origin. She had profound bilateral sensorineural hearing loss, reported to be congenital and heterochromia irides, but no other dysmorphic features or pigmentary changes. Her non-consanguinous parents were normal, as were four siblings. As a child she had suffered fits of unknown origin; CT scan revealed no abnormality. In this regard, W^v homozygotes can show audiogenic seizures, which may be related to the fits described.

Subject D was a 3-year-old Dutch boy who had a 60 dB hearing loss and unilateral heterochromia. All other investigations (ophthalmology, thyroid function, ECG) were normal. He was the only child of normal unrelated parents, born after an uneventful pregnancy and delivery. There was no recorded family history of hearing loss or pigmentary abnormalities.

Mice (Fig. 2) and humans lacking *Slugh*/*SLUG* show neural crest dysfunction. In the human cases this manifests as heterochromia irides and hearing loss, both attributable to patchy absence of melanocytes (1). Hearing loss has not been assessed in the $Slugh^{-/-}$ mice, but we have observed hyperactivity and circling in some mutant animals, a behaviour suggestive of hearing impairment. In the $Slugh^{-/-}$ mice, the phenotypes are influenced by genetic background (6, unpublished observations). Mapping and identifying modifiers of the phenotype may help identify phenotypic determinants in human disease.

The molecular mechanism by which SLUG regulates embryonic development is not known. Thus, we next examined the expression of *Pax3*, *mi* (the mouse homologue of human *MITF*) and *Sox10* in the $Slugh^{-/-}$ mouse model. As shown in Figure 3, *Pax3*, *mi* and *Sox10* mRNA were present in Slug-deficient cells coming from skin. These results are congruent with the observations that, in mouse embryos, *mi* is expressed earlier than *Slugh* in the neural crest where melanocytes

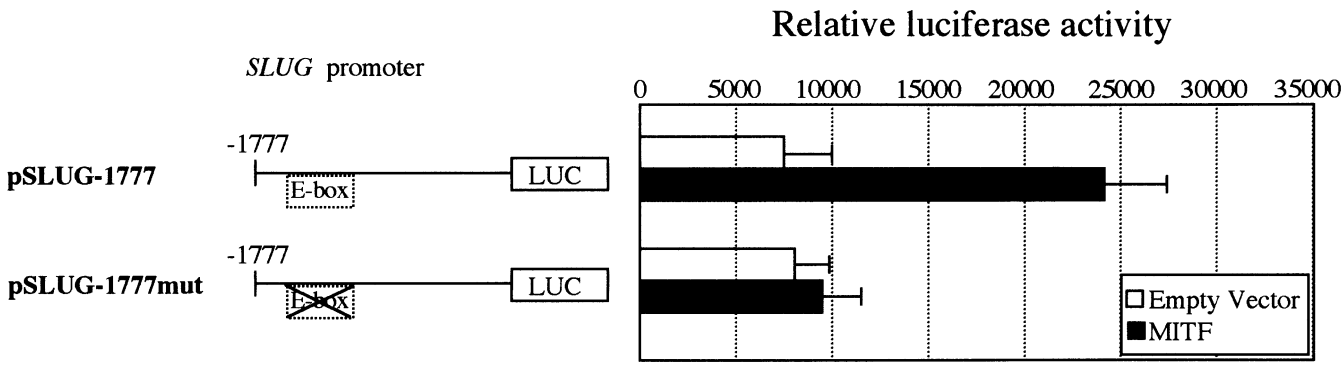

Figure 4. *MITF* transactivates the *SLUG* promoter. Luciferase reporter assays demonstrate E box-dependent responsiveness of the human *SLUG* reporter to *MITF*. The number shown at the left of the reporter constructs denotes the 5′-boundaries (base pairs upstream of the initiation site).

originate (7,9). This led us to hypothesize that *mi*/*MITF* directly regulates SLUG. To test this hypothesis, ~1777 bp of the promoter region of the human *SLUG* gene were cloned upstream of a luciferase reporter gene (pGL3-basic). To directly assess the ability of MITF to activate transcription from DNA sequences present in the *SLUG* promoter, an expression vector containing an *MITF* cDNA was co-transfected into NIH-3T3 cells along with the reporter vector containing the *SLUG* promoter. Co-expression of *MITF* resulted in an approximately three-fold increased in luciferase activity compared with the activity with the empty vector (Fig. 4). These results strongly suggest that MITF interacts with a sequence in the *SLUG* promoter. Indeed, there is a potential MITF binding site, CATGTG, that fits the E box consensus sequence CA[C/T]GTG 1396 bp upstream of the transciptional start. When this E box was mutated, the promoter no longer responded to MITF activation (Fig. 4). It seems likely that failure to activate *SLUG* explains why *MITF* mutations cause Waardenburg syndrome.

Like *mi* mutants, *Kit* and *Scf* (stem cell factor) mutant mice exhibit striking coat colour phenotypes due to loss of viable melanocytes (10–12). These genes co-ordinately modulate the development and survival of the melanocyte lineage. *Kit* functions upstream of *mi* (13) and it has been demonstrated that *Kit* and *mi* interact *in vivo*, resulting in profound melanocyte loss in compound heterozygous mice (14). Thus if Slug mediates the effect of *mi* on melanocyte survival, *Kit* and *Slugh* should genetically interact *in vivo* similarly to *Kit* and *mi*. To examine genetic interactions between *Kit* and *Slugh in vivo*, we generated double heterozygotes for a *Slugh* null allele and the W^v mutation of *Kit*. Complete absence of functional Kit produces mice devoid of melanocytes from birth (Fig. 5D) but heterozygous $W^{v/+}$ mice are born black with occasional white spots (Fig. 5A). Similarly, homozygous mice with the targeted mutation of the *Slugh* gene are born black with occasional white spots (Fig. 2). In the context of $W^{v/+}$ heterozygosity, additional loss of a single *Slugh* allele produced extensive white spotting from birth (Fig. 5B and C). Similar to the genetic cooperativity between *Kit* and *mi*, these observations demonstrate genetic cooperativity between *Kit* and *Slugh* for melanocytes.

In summary, we have shown that mice lacking *Slugh* have patchy deficiency of melanocytes, a phenotype similar to human Waardenburg syndrome. We showed that some human patients with Waardenburg syndrome carry homozygous deletions of *SLUG* as their only detected genetic abnormality, thus defining a recessive form of type 2 WS. Preliminary investigations of the role of *SLUG* in melanocyte development show that it is a downstream target of *mi*/*MITF*, which acts on an E-box sequence in the *SLUG* promoter and that *Slugh Kit* double heterozygous mice show similar melanocyte defects to *mi Kit* double heterozygotes, suggesting that *SLUG* may be the main effector of *mi*/*MITF* action in melanoblasts. The frequency and phenotypic range of humans deficient for *SLUG* remain to be determined.

MATERIALS AND METHODS

Subjects

DNAs from 38 unrelated individuals with WS2 were studied. All patients lack detectable *MITF* gene mutations. The two affected have unaffected parents and are sporadic cases. None of these patients' parents are consanguinous.

Southern blot analysis

Blood was obtained with informed consent and genomic DNAs were prepared from peripheral blood lymphocytes. DNAs were digested with restriction endonucleases as described (15), separated by electrophoresis in 0.8% agarose, transferred to Hybond-N (Amersham). Filters were UV cross-linked and hybridized to a ^{32}P-radiolabelled full-length *SLUG* cDNA probe. DNA loading was monitored by reprobing the filters with a full-length mouse *Kit* cDNA.

Real-time PCR quantification

Real-time quantitative PCR (16) was developed and carried out for the detection and quantitation of both mouse and human *SLUG* genes. The exon 1 primers SLUGF (5′-ATGCCGCGCTCCTTCCT-3′) and SLUGB (5′-TGTGTC-CAGTTCGCT-3′) were used in conjunction with a fluorogenic probe SLUGP [5′-(FAM)-CATTTCAACGCCTCCAARAAG-CC-(TAMRA)-3′]. The fluorogenic probe contained a 3′ blocking phosphate group to prevent probe extension during

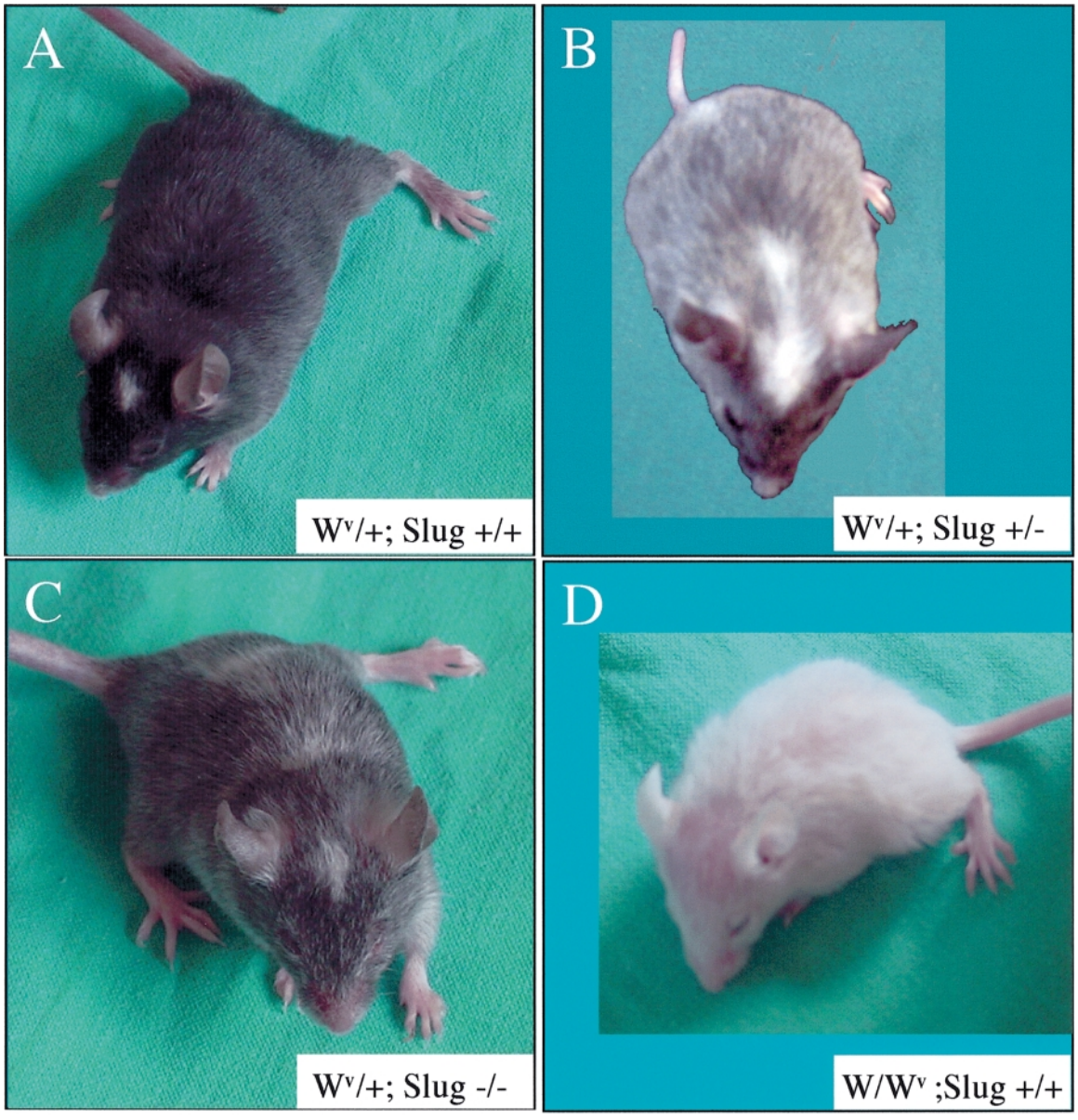

Figure 5. Genetic interaction between *Kit* and *Slugh in vivo*. Mice of the indicated genotypes were crossed and their offspring genotyped. Note that a $W^{v/+}$; $Slugh^{+/+}$ mouse has an almost fully pigmented coat on the dorsal side whereas a 4-week-old $W^{v/+}$; $Slugh^{+/-}$ and a 4-week-old $W^{v/+}$; $Slugh^{-/-}$ mouse show extensive white spotting from birth. The W/W^{v} mouse, which is a compound heterozygote carrying two different mutant alleles of the same gene, is white from birth.

PCR. Fluorogenic PCRs were set up in a reaction volume of 50 µl using the TaqMan PCR Core Reagent kit (PE Biosystems). Fluorogenic probes were custom-synthesized by PE Biosystems. PCR primers were synthesized by Isogen. Each reaction contained 5 µl of 10× buffer; 300 nM of each amplification primer; 25 nM fluorogenic probe; 200 µM of each dNTP; 1.25 U AmpliTaq Gold, 2 mM $MgCl_2$ and 10 ng DNA. DNA amplifications were carried out in a 96-well reaction plate format in a PE Applied Biosystems 5700 Sequence Detector.

Thermal cycling was initiated with a denaturation step of 10 min at 95°C followed by 40 cycles of 95°C for 15 s, 55°C for 30 s and 72°C for 1 min. Multiple negative water blanks were tested and a calibration curve determined in parallel with each analysis. DNAs (10 ng each) from $Slugh^{+/+}$, $Slugh^{+/-}$, and $Slugh^{-/-}$ mice were used for constructing the calibration curve. The β-actin endogenous control (PE Biosystem) was included to relate both mouse and human *SLUG* samples to total genomic DNA in each sample.

Cycle threshold (Ct) readings from $Slug^{+/+}$, $Slug^{+/-}$, and $Slug^{-/-}$ mice were utilized to establish standard curves for each reaction series. The Ct was computed for each sample using Sequence Detection Software (Applied Biosystems) and these settings were automatically used for further computations. Standard curves were generated by plotting the mean of triplicate Ct values versus the log of the *Slug* copy number. The copy numbers for unknown samples were determined by applying the mean Ct value of triplicates to the standard curve. Although equal amounts of DNA were used (10 ng each), a

β-actin endogenous control was included to relate both mouse and human *Slug*/*SLUG* samples to total genomic DNA in each sample.

Analysis of genomic DNA

The three exons of the human *SLUG* gene plus adjacent non-coding and flanking sequences were amplified in duplicate from DNA of patients without *SLUG* deletions by PCR. The nucleotide sequences of at least six independent clones of each were determined.

Mouse crosses

Animals were housed under non-sterile conditions in a conventional animal facility. Mice heterozygous and homozygotes for the $Slugh^{\Delta 1}$ mutation generated by removing the genomic sequences of the entire *Slugh* protein-coding region ($Slugh^{\Delta 1}$ mutant mice) have been described previously (7). W/W^{v} and breeding pairs were obtained from the Jackson Laboratory (Bar Harbor, ME, USA). Heterozygous $Slug^{+/-}$ mice were bred to W^{v} mice to generate compound heterozygotes. F1 animals were crossed to obtain null $Slug^{-/-}$ mice heterozygous for W^{v} deficiency.

Plamid constructs and luciferase assays

The ~1777 bp upstream promoter sequence of *SLUG* was isolated from a P1 clone containing the *SLUG* gene (Genome Systems) and cloned into the luciferase reporter plasmid pGL3-basic (Promega) and termed pSLUG-1777. The pSLUG-1777mut is identical to pSLUG-1777 except that the E-box sequence (CATGTG) in position −1396 is substituted with the mutant sequence gAgGTG (mutated nucleotides in lower case). Human *MITF* cDNA was generated by RT–PCR of total RNA from human melanocytes. Nucleotide sequence was verified by sequencing and the cDNA was cloned into the expression plasmid pEF-BOS (17). For reporter assays, NIH-3T3 cells were transfected using Dual-Luciferase (Promega) with normalization to Renilla luciferase, and mean ± SE was determined from at least three data points. NIH-3T3 cells were maintained in DMEM supplemented with 10% FBS.

Reverse transcription–PCR

To analyse expression of *Slug*, *Pax3*, *mi* and *Sox10* in $Slugh^{+/+}$, $Slugh^{+/-}$ and $Slugh^{-/-}$ mice, RT was performed according to the manufacturer's protocol in a 20 µl reaction containing 50 ng of random hexamers, 3 µg of total RNA and 200 units of Superscript II RNase H^{-} reverse transcriptase (GIBCO/BRL). The sequences of the specific primers were as follows: *Slugh*, sense primer 5′-GCCTCCAAAAAGCCAAACTA-3′ and antisense primer 5′-CACAGTGATGGGGCTGTATG-3′; *Sox10*, sense primer 5′-CATGAACGCCTTCATGGTGT-3′ and antisense primer 5′-AGCTCAGTCACATCAAAGGT-3′; *Pax3*, sense primer 5′-CTAAGATCCTGTGCAGGTAC-3′ and antisense primer 5′-GGTTGCTAAACCAGACCTGC-3′; *Mitf*, sense primer 5′-GTATGAACACGCACTCTCGA-3′ and antisense primer 5′-CTTCTGCGCTCATACTGCTC-3′. Amplification of β-*actin* RNA served as a control to assess the quality of each RNA sample. The PCR products were confirmed by hybridization with specific internal probes.

ACKNOWLEDGEMENTS

We are indebted to members of lab 13 for helpful discussions and specific thanks to Professor R. González-Sarmiento for his unconditional help and support. We are grateful to Dr T. Gridley for the *Slug* mutant mice. This work was supported by DGCYT (SAF2000-0148, and BIO2000-0453-P4-02), Junta de Castilla y León (CSI3/01, and CSI1/02), FIS (01/0114 and PI020138), and NIH grant (1 R01 CA79955-01). A.R.G. is a scholarship holder from CSIC-GLAXO. Work in Manchester was supported by EC grant QLRT-1999-00988 to A.P.R.

REFERENCES

1. Read, A.P. and Newton, V.E. (1997) Waardenburg syndrome. *J. Med. Genet.*, **34**, 656–665.
2. Latchman, D.S. (1996) Transcrption-factor mutations and disease. *N. Engl. J. Med.*, **334**, 28–33.
3. Semenza, G.L. (1994) Transcriptional regulation of gene expression: mechanisms and pathophysiology. *Hum. Mutat.*, **3**, 180–194.
4. Tassabehji, M., Read, A.P., Newton, V.E., Hanus, R., Balling, R., Gruss, P. and Strachan, T. (1992) Waardenburg's syndrome patients have mutations in the human homologue of the Pax-3 paired box gene. *Nature*, **355**, 635–636.
5. Tassabehji, M., Newton, V.E. and Read, A.P. (1994) Waardenburg syndrome type 2 caused by mutations in the human microphthalmia (*MITF*) gene. *Nat. Genet.*, **8**, 251–255.
6. Pérez-Losada, J., Sánchez-Martín, M., Rodríguez-García, A., Flores, T., Sánchez, M^{a}.L., Orfao, A. and Sánchez-García, I. (2002) The zinc-finger transcription factor *SLUG* contributes to the function of the SCF/c-kit signaling pathway. *Blood*, **100**: 1274–1286.
7. Jiang, R., Lan, Y., Norton, C.R., Sundberg, J.P. and Gridley, T. (1998) The *Slug* gene is not essential for mesoderm or neural crest development in mice. *Devl. Biol.*, **198**, 277–285.
8. Liu, X.Z., Newton, V.E. and Read, A.P. (1995) Waardenburg syndrome type 2: phenotypic features and diagnostic aspects. *Am. J. Med. Genet.*, **55**, 95–100.
9. Opdecamp, K., Nakayama, A., Ngugen, M.T., Hodgkinson CA, Pavan, W.J. and Arnheiter, H. (1997) Melanocyte development *in vivo* and in neural crest cell cultures: crucial dependence on the *Mitf* basic–helix–loop–helix–zipper transcription factor. *Development*, **124**, 2377–2386.
10. Chabot, B., Stephenson, D.A., Chapman, V.M., Besmer, P. and Bernstein, A. (1988) The proto-oncogene c-kit encoding a transmembrane tyrosine kinase receptor maps to the mouse W locus. *Nature*, **335**, 88–89.
11. Geissler, E.N., Ryan, M.A. and Housman, D.E. (1988) The dominant-white spotting (W) locus of the mouse encodes the c-kit proto-oncogene. *Cell*, **55**, 185–192.
12. Fleischman R.A. (1993) From white spots to stem cells: the role of the *Kit* receptor in mammalian development. *Trends Genet.*, **9**, 285–290.
13. Hemesath, T.J., Price, E.R., Takemoto, C., Badalian, T. and Fisher, D.E. (1998) MAP kinase links the transcription factor Microphthalmia to Kit signalling in melanocytes. *Nature*, **391**, 298–301.
14. Hou, L., Panthier, J.-J. and Arnheiter, H. (2000) Signaling and transcriptional regulation in the neural crest-derived melanocyte lineage: interactions between *KIT* and *MITF*. *Development*, **127**, 5379–5389.
15. Garcia-Hernandez, B., Castellanos, A., Lopez, A., Orfao, A. and Sanchez-Garcia, I. (1997) Murine hematopoietic reconstitution after tagging and selection of retrovirally transduced bone marrow cells. *Proc. Natl Acad. Sci. USA*, **94**, 13239–13244.
16. Souaze, E., Ntodou-Thome, A., Tran, C.Y., Postene, W. and Forgez, P. (1996) Quantitative RT–PCR: limits and accuracy. *BioTechniques*, **21**, 280–283.
17. Mizushima, S. and Nagata, S. (1990) pEF-BOS, a powerful mammalian expression vector. *Nucl. Acid Res.*, **18**, 5322.